

# Finite element analysis and experimental tests of a permanent magnet synchronous machine for drive train application

**Abstract.** This paper deals with the design and tests of an internal permanent magnet synchronous machine with 12 slots and 10 poles. The machine is analysed under no load condition to estimate the flux linkage and the electromotive force as well as under load condition to calculate the iron core losses, the permanent magnet losses and the output power by utilizing the transient finite element analysis. Several simulation results under no load condition e.g. open circuit voltage and under load condition e.g. torque are compared with those of the experiment to validate the electromagnetic simulation model and to investigate the machine's characteristics.

**Streszczenie:** W artykule opisano projekt i badania silnika synchronicznego z magnesami trwałymi z 12 szczelinami i 10 biegunami. Silnik analizowano w stanie jałowym w celu określenia strumienia magnetycznego oraz pod obciążeniem w celu określenia strat i mocy wyjściowej. Przeprowadzono symulację i wyniki porównano z danymi eksperymentalnymi. Analiza metodą elementów skończonych oraz badania silnika synchronicznego o magnesach trwałych przeznaczonego do zastosowania w pojeździe kolejowym

**Keywords:** interior permanent magnet synchronous machine, finite element analysis, magnet losses, iron losses, drive train.

**Słowa kluczowe:** silnik synchroniczny, metoda elementów skończonych, straty

## Introduction

The aim of this work is the design and tests of an interior permanent magnet synchronous machine (IPMSM) for electrical drive train application. The main requirements of the designed and tested machine are high efficiency, recuperation of the brake energies, low manufacturing costs and low weight. To fulfil these demands a high-integrated power transmission system is designed under realistic conditions and tested on the test bench. The highly integrated system consists of an inverter and IPMSM. The integration of the inverter on the electrical machine decreases the cooling requirements, since electrical machine and inverter are connected to the same water cooling system. Moreover, the high integration reduces the quantities of the electrical components, e.g. connections, plugs, seals, and simplifies the technical design of the individual sub-assemblies. This approach obtains benefits in terms of decreasing volume and weight of the drivetrain. The benefits of the highly-integrated system are essential especially for small city cars and industry logistic applications, where the available space for the drive train is limited and the vehicles has to be manufactured with a low nominal weight. Additionally, the high integration of the drivetrain's components decrease the production costs and improves the economic manufacturing of electrical vehicles.

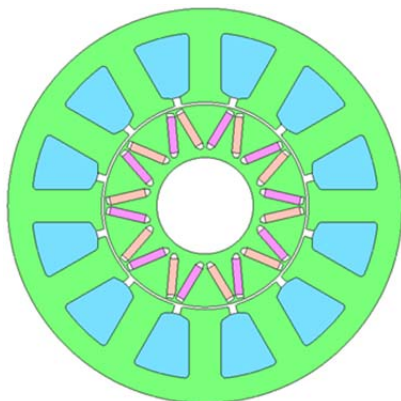


Fig. 1. V-shape magnet inside the rotor

## IPMSM characteristics

A fractional-slot concentrated-winding (FSCW) 12-slot/10-pole IPMSM has been designed by means of finite element simulation and verified by experimental tests. The usage of

FSCW has benefits in terms of high copper fill ratio, high efficiency and small phase resistance, due to the short end winding [1-3]. Moreover, FSCW machine offers numerous advantages in terms of low cogging torque, high efficiency and power density [2], [4]. The machine in this work is designed to deliver a maximum power of 25 kW and for operation speed up to 9000 1/min. The rotor core and stator core are laminated and the magnets are arranged in v-shape inside the rotor as shown in Fig 1. Table 1 shows the rated parameters of the IPMSM machine.

Table 1: Rated Parameters of the IPMSM machine

DC Supply Voltage	250 V
RMS maximum current	140 A
Rated speed	3750 1/min
Maximum speed	9000 1/min
Maximum Power	25 kW
Maximum Torque	65 Nm

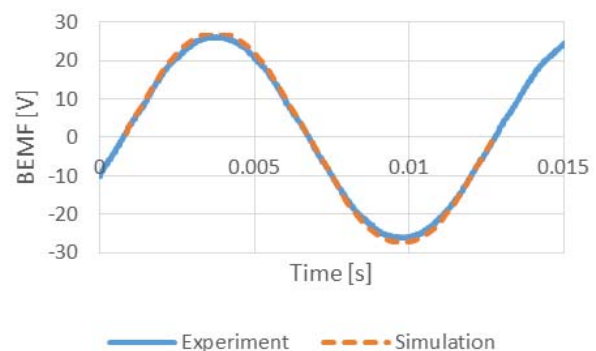


Fig. 2. Measured and calculated BEMF waveforms for one phase at 1000 1/min

## Open circuit voltage tests

In the first instance, no load tests are executed to measure the open circuit back electromotive force (BEMF). Under no load condition, the load machine drives the test machine with constant speed and the phase BEMF is measured. Fig. 2 shows the measured BEMF for one phase compared to the BEMF from the FEA at 1000 1/min and demonstrates the good matches of the waveform shape and magnitude with small discrepancy. The Amplitude of the predicted fundamental BEMF is approx. 4% lower than that measured in the machine. The waveform of the BEMF

draws near to the sinusoidal shape as can be seen from Fig. 2 and allows a good ability to carry the load current. Fig. 3 shows the harmonic spectrum of the simulated and measured BEMF at 1000 1/min indicating the fundamental voltage and the low values of the higher harmonics.

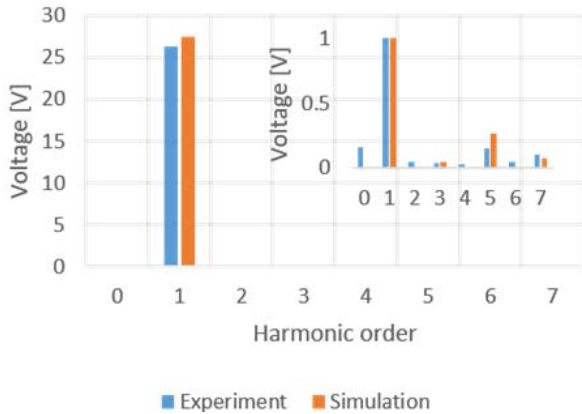


Fig. 3. Harmonic spectrum of the measured and predicted phase BEMF at 1000 1/min

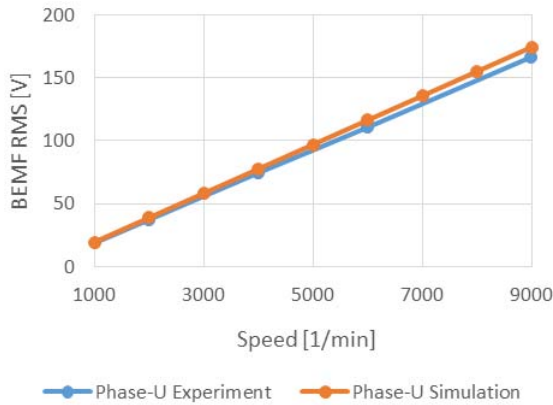


Fig. 4. RMS values of the measured and simulated BEMF versus speed

The machine is tested up to 9000 1/min. Fig. 4 shows the root mean square (RMS) values of the simulated and measured BEMF across the whole speed range between 1000 and 9000 1/min.

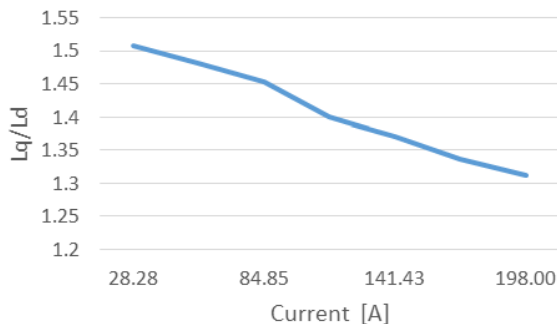


Fig. 5.  $L_q/L_d$  ratio depending on the current magnitude

### Machine inductances

In the IPMSM, the magnets are buried inside the rotor core lamination, which leads to increase the saliency, resulting in improvement of the flux-weakening capabilities. The inductances  $L_q$  and  $L_d$  are calculated to determine the saliency and to investigate the machine's performance in the flux-weakening region. Moreover, knowledge on the values of  $L_q$  and  $L_d$  is required to calculate the reluctance

torque. Fig. 5 shows the ratio  $L_q/L_d$  depending on the current magnitude.

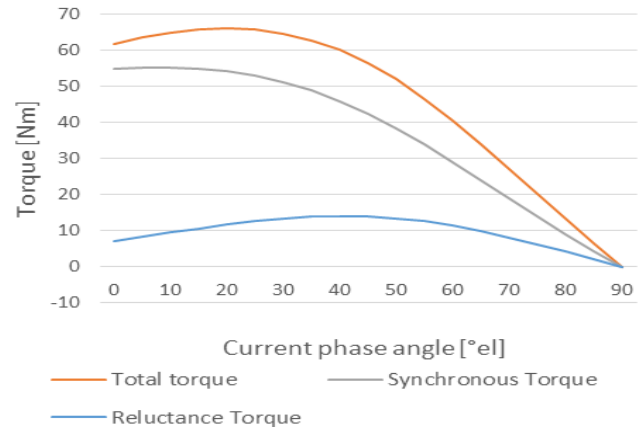


Fig. 6. Torque versus current phase angle

### Machine performance under load condition

At the rated speed and maximum current, the torque is simulated for different current angle to determine the optimum phase angle for maximum torque. Fig. 6 shows the total torque, the synchronous torque and the reluctance torque as a function of the current phase angle. The simulation of the reluctance torque was done using the frozen permeability function of the FE-Software JMAG [5]. The maximum torque per ampere (MTPA) is also given for the current angle  $20^\circ$  as can be seen from Fig. 6.

In the constant torque region, the current is constrained according to the capabilities of the power inverter and the cooling system. The operating points in this range are simulated according to the above-illustrated MTPA characteristics. In the flux-weakening region, the operation with the maximum current is dispensable and is decreased to decrease the torque and achieve a constant power as speed increase. Moreover, the operation with the full load in the flux- weakening region leads to higher iron core and magnet losses. In this region, the q-axis current decreases to decrease the torque, while the d-axis current is controlled due to the flux weakening to constrain the motor voltage at constant value under the limit as speed increases. Fig. 7 shows the peak values of the phase current and the d-axis and q-axis current components of the studied operating points in the constant torque region as well in the flux weakening region. The determination of the d-axis and q-axis currents is crucial and influence not only the torque and power characteristics, but although the development of the losses as speed increase.

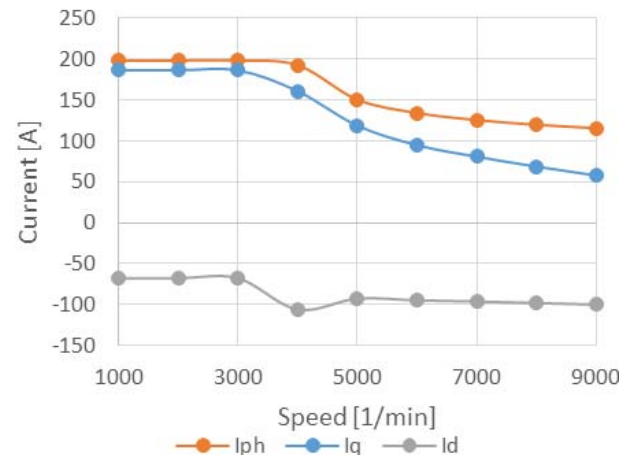


Fig. 7. Q-axis and d-axis current over the speed range up to 9000 1/min

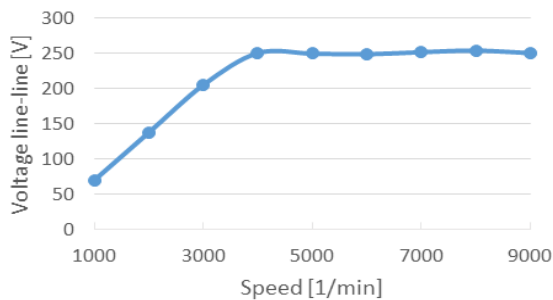


Fig. 8. Line-line voltage versus speed

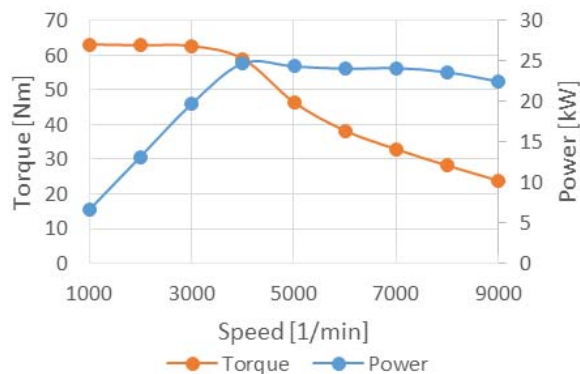


Fig. 9. Power and torque versus speed

Fig. 8 shows the simulated motor line-line voltage as a function of the speed and illustrate the constant voltage required in the flux-weakening region. The amplitude of the motor line-line voltage is limited to 250V and is lower than the maximum inverter voltage. Under load conditions, the machine is simulated with the 2D FEM model by sinusoidal current excitation. The simulated torque and power characteristics of the 25 kW IPMSM across the whole speed range are shown in Fig. 9.

The performance of the machine is although investigated by utilising the 3-D FE transient analysis under no load condition, as well with full load. The simulation of The BEMF with the 3-D model does not shows any noticeable difference compared to the 2-D analysis, where the load analysis indicate some discrepancy. The calculated torque with the 3-D model is 4% smaller than that of the 2-D model. One of the sources this discrepancy is the consideration of the flux leakage, especially in the axis direction. Since the active length of the designed machine is smaller than the outer diameter, the flux leakage has a significant influence on the machine's performance. Fig. 10 shows the simulated torque according to the 2-D and 3-D-model compared to the measured one. The 3-D simulated torque is approx. 5.6% higher than that measured. One source of this discrepancy is the neglecting of the mechanical losses (bearings, seal and friction losses) in the simulation. Moreover, the current was excited with the pulse width modulation (PWM) on the experimental setup, which can lead to higher current harmonics and additional losses. The experimental setup is shown in Fig. 11.

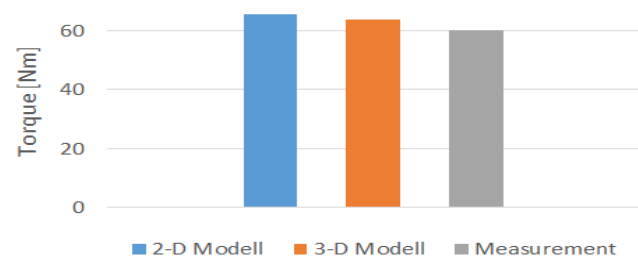


Fig. 10. Predicted and measured output torque

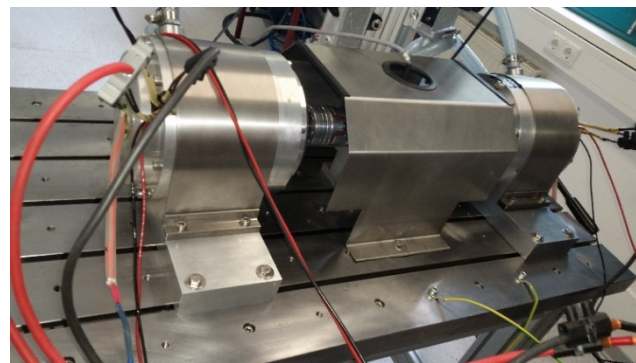


Fig. 11. Experimental setup

### Copper losses

The copper losses are proportional to the square of the phase current and indicate the same current variation. The copper losses are dominant in the constant torque range due to the constant load current. In the flux-weakening region, the current decreases from the nominal speed to decrease the torque and the copper losses decrease as well as can be shown from Fig. 12.

### Iron Losses

The iron losses in permanent magnet synchronous machine occur according to the fundamental magnetic field and to their harmonics. Moreover, the harmonic magnetomotive forces of the permanent magnet and the stator slots are other sources for iron losses [6], [7]. Another source of the iron losses is the harmonic of the pulse width modulated (PWM) inverters, when the current is excited by a PWM-inverter [6], [7]. The occurred losses across the total speed range are investigated in order to establish the efficiency and the output power of the electrical machine. The simulation of the iron losses is done by the transient numerical 2D-FEA takes into account the time variation of the magnetic flux. Fig. 12 shows the iron core losses estimated according to the current characteristics in Fig. 7. The stator and rotor core losses include both eddy current and hysteresis losses. Both are dominant in the flux-weakening region, due to the increased speed, as expected. The eddy current losses are proportional to the square of the frequency and the hysteresis losses increase linear with the frequency.

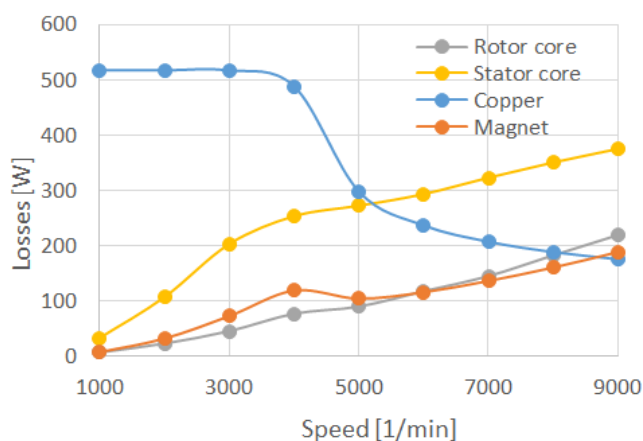


Fig. 12. Predicted losses of the IPMSM machine

### Magnet eddy current losses

The magnet eddy-current losses occurs in FSCW-PM for several reasons, which are for instance the slot harmonics and the carrier harmonics of PWM inverters [8]. A known method to reduce these losses is the segmentation of each magnet into multiple segments in the axial direction, as well

in the circumferential direction. In the developed machine, each magnet is segmented into two segments in the axial direction, and an insulating layer exists between the two adjacent segments. Due to the magnet segmentation, the eddy current path in the axial direction is broken as can be seen from Fig. 13, and the magnetic resistance increases resulting in lower magnet losses [9]. In this work, the eddy current losses in the permanent magnets are predicted by utilizing the 3-D transient FEA.

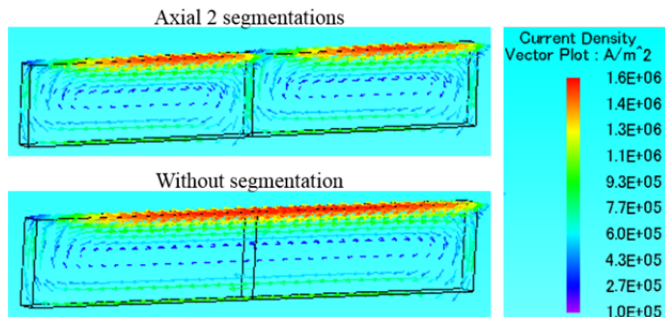


Fig. 13. Magnet eddy current density

The magnet eddy current losses depends on the load current and frequency. At constant load, the magnet losses are proportional to the square of the frequency (speed) as can be shown from Fig. 12. This is the case in the constant torque region. After the corner point at 5000 1/min, the current decreases due to the flux-weakening, resulting in decreasing of the magnet losses as well as shown in Fig. 12.

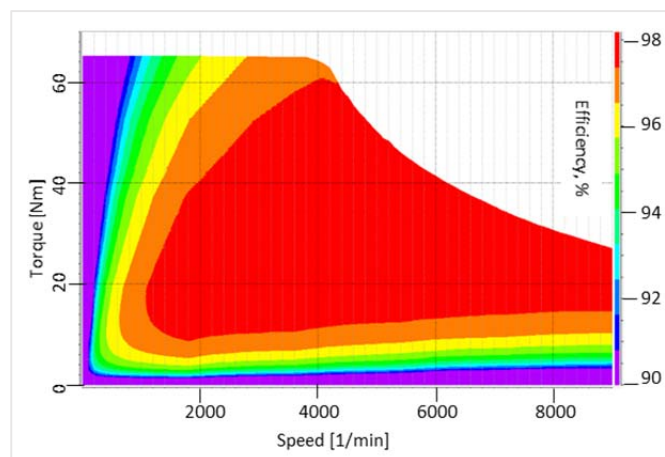


Fig. 14. Efficiency map of the 25 kW machine

The maximum losses in the permanent magnet material are obtained at the maximum speed 9000 1/min. At this operating point, the total permanent magnet losses are calculated as 189 W. This losses are 12.5% lower than the magnet losses without segmentation. The predicted total losses at the corner speed are 980 W resulting in an efficiency of 96.7%. This losses does not include the mechanical losses. Fig. 14 shows the efficiency map simulated with the software JMAG-RT.

## Conclusions

In this work a concentrated winding 25 kW IPMSM machine has been designed for drive train application and successfully tested. The designed machine has an efficiency over 96.7% at the nominal operation point. According to the winding configuration, the machine has a high slot fill ration over 48%, resulting in a low phase resistance ( $8.8m\Omega$ ) and a permissible copper current density of  $10 A/mm^2$  at the maximum current. The electromagnetic design of the IPMSM has been carried out taking into consideration their control strategy in the constant torque range as well as in the flux-weakening range, and the demands of the inverter. This procedure is required to achieve high performance of the complete drive train. Especially the inductances are essential for the inverter design and motor control. The machine's quantities e.g. torque and losses has been calculated depending on the d-axis and q-axis current components. Experimental tests has been carried out and demonstrate a good agreement with the FEA results.

Authors: Kassem ROUMANI<sup>1</sup>, Waldemar STEPHAN<sup>2</sup>, Benedikt SCHMUELLING<sup>1</sup>

University of Wuppertal, E-Mobility Research Group, Germany (1),  
Online Engineering GmbH, Germany (2)  
roumani@uni-wuppertal.de

## REFERENCES

- [1] A.M. EL-Refaie, J.P. Alexander, S. Galioto, P.B. Reddy, K. Huh, P. Bock, X. Shen, "Advanced High-Power-Density Interior Permanent Magnet Motor for Traction Applications," IEEE Trans. Ind. Appl., vol. 50, no. 5, pp. 3235 – 3248, September/October 2014.
- [2] Y. Yokoi 1, T. Higuchi, Y. Miyamoto, "General formulation of winding factor for fractional-slot concentrated winding design," IET Electric Power Applications, vol.10, no. 4, pp. 231 – 239, 21 April 2016.
- [3] K. Shin, J. Choi, H. Cho, „Characteristic Analysis of Interior Permanent- Magnet Synchronous Machine with Fractional-Slot Concentrated Winding Considering Nonlinear Magnetic Saturation," IEEE Transactions on Applied Superconductivity Vol. 26, no. 4, pp. 1051-8223, 19 Januar 2016.
- [4] G. Choi, T. M. Jahns, "Reduction of Eddy-Current Losses in Fractional- Slot Concentrated-Winding Synchronous PM Machines," IEEE Transactions on Magnetics, vol. PP, no. 99, 12 January 2016.
- [5] www.jmag-international.com
- [6] Han, S. H., Jahns, T. M., Zhu, Z. Q., (2010), "Analysis of Rotor Core Eddy-Current Losses in Interior Permanent-Magnet Synchronous Machines," IEEE transactions on industry applications, vol. 46, no. 1. pp. 196-205.
- [7] Yamazaki, K., Ishigami, H., "Reduction of Harmonic Iron Losses in Interior Permanent Magnet Motors by Optimization of Rotor Structures," International Conference on Electrical Machines and Systems ICEMS 2008, Wuhan, pp.2870 – 2875.
- [8] Yamazaki, K., Fukushima, Y., (2011) "Effect of Eddy-Current Loss Reduction by Magnet Segmentation in Synchronous Motors with Concentrated Windings," IEEE Transactions on Industry Applications vol. 47, no. 2 pp. 779 – 788.
- [9] Hendershot, J.R., Miller, T.J.E., "Design of Brushless Permanent-Magnet Machines". USA: Motor design books LLC, 2010.